

AD/A-000 434

NON-ELASTIC DEFORMATION OF POLY-
CRYSTALS WITH A LIQUID BOUNDARY
PHASE

F. F. Lange

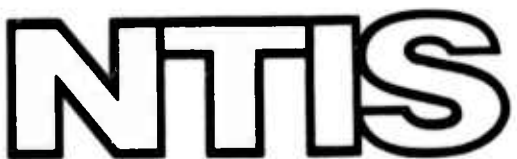
Westinghouse Research Laboratories

Prepared for:

Office of Naval Research
Advanced Research Projects Agency

23 September 1974

DISTRIBUTED BY:



National Technical Information Service
U. S. DEPARTMENT OF COMMERCE

**NON-ELASTIC DEFORMATION OF POLYCRYSTALS
WITH A LIQUID BOUNDARY PHASE**

Technical Report #1, September 23, 1974

**Westinghouse Electric Corporation
Research and Development Center**

Contract Number N00014-74-C-0284

**Sponsored by the Advanced Projects Agency
ARPA Order Number 2697
Program Code Number 01269**

**Scientific Officer: Dr. A. M. Diness
Office of Naval Research**

**Principal Investigator: Dr. F. F. Lange
(412) 256-3684**

Effective Date of Contract: April 1, 1974

Contract Expiration Date: June 30, 1975

Amount of Contract: \$79,904

Form Approved, Budget -- No. 22-R0293

**The views and conclusions contained in this document
are those of the authors and should not be interpreted
as necessarily representing the official policies, either
expressed or implied, of the Advanced Research Projects
Agency of the U. S. Government.**

Reproduced by
**NATIONAL TECHNICAL
INFORMATION SERVICE**
U S Department of Commerce
Springfield VA 22151

DISTRIBUTION STATEMENT A

**Approved for public release;
Distribution Unlimited**



UNCLASSIFIED

Security Classification

ADA-000-434

DOCUMENT CONTROL DATA - R&D

(Security classification of title, body of abstract and indexing annotation must be entered when the overall report is classified)

1. ORIGINATING ACTIVITY (Corporate author)	2a. REPORT SECURITY CLASSIFICATION UNCLASSIFIED
Westinghouse Research & Development Center	2b. GROUP

3. REPORT TITLE

NON-ELASTIC DEFORMATION OF POLYCRYSTALS WITH A LIQUID BOUNDARY PHASE

4. DESCRIPTIVE NOTES (Type of report and inclusive dates)

Technical Report

5. AUTHOR(S) (Last name, first name, initial)

Lange, F. F.

6. REPORT DATE September 23, 1974	7a. TOTAL NO. OF PAGES 49	7b. NO. OF REFS 18
8a. CONTRACT OR GRANT NO. N00014-74-C-0284 <i>new</i>	9a. ORIGINATOR'S REPORT NUMBER(S) 74-9D4-POWDR-R1	
9. PROJECT NO. c. d.	9b. OTHER REPORT NO(S) (Any other numbers that may be assigned this report) None	
10. AVAILABILITY/LIMITATION NOTICES Reproduction in whole or in part is permitted for any purpose of the U. S. Government. Distribution of this document is UNLIMITED.		
11. SUPPLEMENTARY NOTES	12. SPONSORING MILITARY ACTIVITY Advanced Research Projects Agency	

13. ABSTRACT A conceptual view is taken to understand the deformation behavior of a polycrystal with a liquid (or a quasi-elastic) boundary phase. The analysis is based on the theories of liquid adhesives, the fracture of liquids and the concepts of fracture mechanics. It is shown that boundary separation rather than boundary sliding is the step that controls the deformation rate. Using this principal result, it is shown that the deformation behavior of a polycrystalline material with a viscous boundary phase is controlled by the flow characteristics, the volume content of the boundary phase and the microstructure features of the polycrystal (viz., voids, solid inclusions and cracks). Polycrystalline materials with a viscous boundary phase will exhibit a much greater rate of deformation in tension than in compression.

UNCLASSIFIED

Security Classification

14 KEY WORDS	LINK A		LINK B		LINK C	
	ROLE	WT	ROLE	WT	ROLE	WT
phase Newton deformation crystals creep solid liquid cracks voids separation sliding growth boundaries						
INSTRUCTIONS						
1. ORIGINATING ACTIVITY: Enter the name and address of the contractor, subcontractor, grantee, Department of Defense activity or other organization (corporate author) issuing the report.	imposed by security classification, using standard statements such as:					
2a. REPORT SECURITY CLASSIFICATION: Enter the overall security classification of the report. Indicate whether "Restricted Data" is included. Marking is to be in accordance with appropriate security regulations.	<ul style="list-style-type: none"> (1) "Qualified requesters may obtain copies of this report from DDC." (2) "Foreign announcement and dissemination of this report by DDC is not authorized." (3) "U. S. Government agencies may obtain copies of this report directly from DDC. Other qualified DDC users shall request through ." 					
2b. GROUP: Automatic downgrading is specified in DoD Directive 5200.10 and Armed Forces Industrial Manual. Enter the group number. Also, when applicable, show that optional markings have been used for Group 3 and Group 4 as authorized.	<ul style="list-style-type: none"> (4) "U. S. military agencies may obtain copies of this report directly from DDC. Other qualified users shall request through ." (5) "All distribution of this report is controlled. Qualified DDC users shall request through ." 					
3. REPORT TITLE: Enter the complete report title in all capital letters. Titles in all cases should be unclassified. If a meaningful title cannot be selected without classification, show title classification in all capitals in parenthesis immediately following the title.	If the report has been furnished to the Office of Technical Services, Department of Commerce, for sale to the public, indicate this fact and enter the price, if known.					
4. DESCRIPTIVE NOTES: If appropriate, enter the type of report, e.g., interim, progress, summary, annual, or final. Give the inclusive dates when a specific reporting period is covered.	11. SUPPLEMENTARY NOTES: Use for additional explanatory notes.					
5. AUTHOR(S): Enter the name(s) of author(s) as shown on or in the report. Enter last name, first name, middle initial. If military, show rank and branch of service. The name of the principal author is an absolute minimum requirement.	12. SPONSORING MILITARY ACTIVITY: Enter the name of the departmental project office or laboratory sponsoring (paying for) the research and development. Include address.					
6. REPORT DATE: Enter the date of the report as day, month, year; or month, year. If more than one date appears on the report, use date of publication.	13. ABSTRACT: Enter an abstract giving a brief and factual summary of the document indicative of the report, even though it may also appear elsewhere in the body of the technical report. If additional space is required, a continuation sheet shall be attached.					
7a. TOTAL NUMBER OF PAGES: The total page count should follow normal pagination procedures, i.e., enter the number of pages containing information.	It is highly desirable that the abstract of classified reports be unclassified. Each paragraph of the abstract shall end with an indication of the military security classification of the information in the paragraph, represented as (TS), (S), (C), or (U).					
7b. NUMBER OF REFERENCES: Enter the total number of references cited in the report.	There is no limitation on the length of the abstract. However, the suggested length is from 150 to 225 words.					
8a. CONTRACT OR GRANT NUMBER: If appropriate, enter the applicable number of the contract or grant under which the report was written.	14. KEY WORDS: Key words are technically meaningful terms or short phrases that characterize a report and may be used as index entries for cataloging the report. Key words must be selected so that no security classification is required. Identifiers, such as equipment model designation, trade name, military project code name, geographic location, may be used as key words but will be followed by an indication of technical context. The assignment of links, rules, and weights is optional.					
8b, 8c, & 8d. PROJECT NUMBER: Enter the appropriate military department identification, such as project number, subproject number, system numbers, task number, etc.						
9a. ORIGINATOR'S REPORT NUMBER(S): Enter the official report number by which the document will be identified and controlled by the originating activity. This number must be unique to this report.						
9b. OTHER REPORT NUMBER(S): If the report has been assigned any other report numbers (either by the originator or by the sponsor), also enter this number(s).						
10. AVAILABILITY/LIMITATION NOTICES: Enter any limitations on further dissemination of the report, other than those						

UNCLASSIFIED

Security Classification

RM 35055

1. INTRODUCTION

Grain boundary sliding first comes to mind in relating a viscous boundary phase with deformation. Because individual grain pairs are constrained by surrounding grains, grain boundary sliding is restricted unless either the grains themselves can accommodate the deformation produced by the sliding or the boundaries can develop cavities (viz., voids or cracks). Present concepts relating boundary sliding to the deformation behavior of polycrystalline materials allow some accommodation to take place by either elastic or plastic deformation within the grains.^(1,2) As pointed out by Raj and Ashby,⁽³⁾ elastic deformation does not result in sufficient accommodation to allow boundary sliding. Thus, if the formation of cavities are to be prevented, the grains must exhibit plastic deformation by dislocation and/or diffusional processes.

Grain boundary cavities are frequently found in materials that have been forced to exhibit large deformations prior to fracture. Mechanisms and theories have been proposed to account for the formation and the growth of these cavities,^(1,2) but no account has been taken for either the presence or the properties of a grain boundary phase. This is understandable since the models and the theories have been proposed to explain boundary cavitation in metals which were presumed not to contain a grain boundary phase.

In the present theory, the expected deformation behavior of a polycrystalline material containing a viscous grain boundary phase will be examined with respect to the volume fraction and the properties of the boundary phase. It is assumed that the grains do not exhibit any plastic deformation. Most of the analytical treatment will be concerned with the behavior of grains separated with a Newtonian liquid, but the general case of quasi-elastic boundary phases will also be discussed. The analysis of this material model is based on the theories of liquid adhesives, the fracture of liquids and the concepts of fracture mechanics. It will be shown that boundary separation rather than boundary sliding is the step that controls the deformation rate. Based on this principal result, it will be shown that the deformation behavior of a polycrystalline material with a viscous boundary phase is controlled by the flow characteristic and the volume content of the boundary phase, microstructural features of the polycrystal (viz., voids, solid inclusions and cracks), and the mode in which the stress is applied (e.g., tension vs compression).

2. BOUNDARY SLIDING vs BOUNDARY SEPARATION

The model used to analyze the deformation behavior of a polycrystalline material with a viscous boundary phase is shown in Fig. 1. It consists of cube-shaped grains, which are assumed to exhibit neither plastic deformation nor rotation, separated by a Newtonian liquid of thickness s_0 . Other features as, for example, the presence of vapor bubbles within the boundary phase, will be brought into the model at the appropriate point.

As discussed in the introduction, deformation by grain boundary sliding cannot be accommodated with elastic grains unless boundary separation occurs. For a polycrystal with a liquid boundary phase, boundary separation requires either the flow of liquid to occupy the increased volume between the separating grains or the growth of a vapor bubble. In either case, boundary separation requires a resolved tensile stress across the grains. Boundary sliding requires resolved shear stresses.

The resistance of grain pairs to sliding and separation can be examined separately as shown in Fig. 2 using two grains with cube edges D separated by a Newtonian liquid with a viscosity η acted upon by a force F . Figure 2a represents the case for boundary sliding, i.e., the sliding of each grain with respect to the surrounding grains. For this case, the liquid between the grains is missing so that the volume

increase between the separating grains is not restricted by either the flow of liquid or the growth of a vapor bubble. Figure 2b represents the case for boundary separation, where the only liquid present is between the boundaries to be separated.* In both cases, the strain in the direction of force (F) is $\epsilon \equiv (s - s_0)/(D + s_0)$ where s_0 is the initial separation distance and s is the separation between the grain pair after a period, t .

The classical equation that defines the rate of sliding (ds/dt) of one surface of area A separated by a distance s_0 from another by a Newtonian liquid is⁽⁴⁾

$$\frac{ds}{dt} = \frac{s_0 F}{\eta A} . \quad (1)$$

Substituting $ds = (D + s_0)d\epsilon$ and the shear stress $\tau = F/A$, the strain rate ($\dot{\epsilon}$) for boundary sliding (Fig. 2a) is given by

$$\dot{\epsilon} = \frac{s_0}{(D + s_0)} \frac{\tau}{\eta} \quad (2)$$

By integrating this expression and substituting^{**} $s_0 = xD$, the time required to produce a certain strain in the direction of applied force is given by

$$t = \frac{(x + 1)\eta}{x\tau} \epsilon . \quad (3)$$

* The condition of the limited amount of liquid between grain pairs is more representative of a polycrystalline material as discussed in the next section. The grain pair in Fig. 2a can also be surrounded by a large reservoir of liquid. Expressions⁽⁹⁾ developed for this condition only differ from that given in Eq. (4) by a factor of 2.

** The relation between s_0 and D depends on the volume fraction of the liquid phase, V_L . As shown in Appendix A, $x \approx V_L/(3(1-V_L))$ for the case of cube-shaped grains.

Solutions for the separation of boundaries with a sandwiched liquid (Fig. 2b) are found in the literature on adhesion. (5,6,7)

Neglecting the capillary forces by assuming the surface tension of the liquid is zero,* Healey's⁽⁸⁾ solution is

$$\frac{ds}{dt} = \frac{2\pi s^5}{3\eta V^2} F. \quad (4)$$

By substituting the tensile stress across the boundary $\sigma = F/D^2$, the expression for the liquid's volume, $V = D^2 s_0$, $ds = (D + s_0) d\epsilon$, and $s_0 = xD$, an expression for the strain rate in the direction of force is obtained for an arbitrary separation distance (s):

$$\dot{\epsilon} = \frac{2\pi x^3 s^5}{3(x+1)\eta s_0^5} \sigma \quad (5)$$

By integrating the above expression, the time required to produce a certain strain in the direction of the applied force is given by

$$t = \frac{3\eta}{8\pi x^2 \sigma} \left[1 - \frac{1}{\left(\frac{1}{x} + 1 \right) \epsilon + 1} \right]^4 \quad (6)$$

which can be approximated by

$$t = \frac{3\eta (x+1)}{8\pi x^3 \sigma} \left[\frac{\epsilon}{\left(\frac{1}{x} + 1 \right) \epsilon + .25} \right] \quad (7)$$

when $\epsilon < 0.1$.

By comparing Eqs. (3) and (7), it can be shown that when $x \ll 1$ (the case where the volume fraction of the liquid phase is small) and when $\epsilon \leq .1$, a much longer period is required to produce the same strain by boundary separation than by boundary sliding. Similar strains are only produced by both phenomenon in the same period when either the volume

* Surface tension can be brought into this relation, (5) but its effect is not necessary for the argument.

fraction of the liquid phase is large or after a long period of time when the grains become separated by large distances. Thus, when the two phenomena are allowed to operate concurrently as shown in Fig. 2(c), it can be concluded that the deformation rate of the grain pair will be limited to the rate in which the boundaries can separate due to the applied tensile stress across the boundary. That is, boundary sliding is an incidental phenomenon whereas boundary separation is the rate limiting step.*

The deformation rate of the grain pair shown in Fig. 2c is therefore defined by Eq. (5). Similar equations are reported in Appendix B for the case where the boundary phase is either a non-Newtonian liquid or a Bingham solid.

* This conclusion is quickly reached by the casual experiment of separating two glass plates which are sandwiched together with either water or grease. It is easier to slide the plates than to pull them apart.

3. NEED FOR VAPOR-LIQUID SURFACES

The free flow of liquid between the boundaries is necessary for separation. The model used to examine boundary separation (Fig. 2b) assumed that the volume of liquid between the boundaries remained constant. As the boundaries separated, the vapor-liquid interface moved inward to account for the increased volume between the boundaries. A free flow of liquid would also occur if the grain pair were immersed in a large reservoir of liquid. In this case, the liquid in the reservoir moves to occupy the increased volume between the separating boundaries. The strain rate equation for this case differs from Eq. (5) by a factor of 2. ⁽⁹⁾

Boundaries that are located on either external or internal surfaces of a polycrystalline body would resemble the case shown in Fig. 2b, i.e., the flow of liquid between the boundaries is unrestricted due to the movement of the vapor-liquid interface. Separating boundaries that are remote from a free surface would have to either contain a small vapor bubble (which would grow during separation) or borrow liquid from the surrounding boundaries.

The borrowing of liquid or the free flow of liquid from one boundary to another requires that some boundaries approach one another while others separate. Boundary approach requires compressive stresses. Although compressive stresses can arise across some boundaries in a

polycrystalline material placed in tension, Eq. (5) illustrates that the rate of boundary approach ($s/s_0 < 1$) due to a compressive stress ($-\sigma$) is much smaller than the rate of boundary separation ($s/s_0 > 1$) due to a tensile stress (σ). Thus, for the ideal case where all boundaries are initially separated by a distance s_0 (Fig. 1), liquid is unlikely to flow from boundary to boundary. This restrictive flow of liquid requires that boundaries remotely located from free surfaces have a vapor bubble which can grow and allow the free flow of liquid between the separating boundaries. As discussed in the next section, the criterion for the growth of vapor bubbles depends on the applied tensile stress, the size of the bubble and the surface energy of the liquid.

4. CRITICAL STRESS FOR THE GROWTH OF VAPOR BUBBLES

A confined liquid subjected to a negative pressure (i.e., a tensile stress) is metastable; it will change to a two phase, liquid plus vapor, system. The vapor state takes the form of bubbles that grow until the liquid fractures. The growth of vapor bubbles was analyzed by Fisher⁽¹⁰⁾ in a manner similar to that introduced by Griffith⁽¹¹⁾ for analyzing the fracture of solids. Fisher showed that for a given tensile stress, only vapor bubbles greater than a critical size will grow. The relation between the critical bubble diameter (d_c) and the applied tensile stress (σ) is given by

$$d_c = \frac{4\gamma}{\sigma} , \quad (8)$$

where γ is the vapor-liquid surface energy. Bubbles with diameters less than d_c require free energy for further growth, whereas those with larger diameters grow spontaneously with a decreasing free energy. By rearranging this expression, it can be seen that a bubble of diameter d requires a stress \geq than a critical stress (σ_c):

$$\sigma_c \geq \frac{4\gamma}{d} . \quad (9)$$

The growth of smaller bubbles requires larger stresses. When the criterion for bubble growth is applied to the separation of grain boundaries remote to a free surface, two conditions must be satisfied.

First, a vapor bubble must either pre-exist or nucleate at the boundary. As pointed out by Fisher,⁽¹⁰⁾ unless the liquid has a zero contact angle with the solid, the pre-existence of a vapor bubble is inevitable. Even for perfect wetting, a small region of positive contact impurity is sufficient for the existence of a vapor bubble. Lacking this, the vapor bubble must nucleate due to a thermally activated process.

The second condition is that the tensile stress across the boundary is $\geq \sigma_c$. The magnitude of the critical stress can be estimated using Eq. (9) and a few assumptions. Assuming that $\gamma = 0.35 \text{ J/m}^2$ (a value for many silicate glasses⁽¹²⁾ at 1200°C), $d = s_0 \approx 0.02 \mu\text{m}$ (for a grain size of $1 \mu\text{m}$, and $V_\ell = 5\%$ -- see Eq. (3a) in Appendix I), the smallest critical stress is $\sigma_c = 60 \text{ MN/m}^2$ (8700 psi). For this case, grain pairs remote to a free surface will not begin to separate unless the applied tensile stress is $\geq 60 \text{ MN/m}^2$. It should be noted that since $d \leq s_0$, and s_0 depends on grain size for a given liquid content, a lower critical stress is required to separate larger grain size materials.

5. EFFECT OF STRESS CONCENTRATORS

As discussed in a previous section, grain pairs that are located on a surface are free to separate at any tensile stress. When the surface is flat, the tensile stress across the properly oriented boundary is equal to the applied tensile stress (σ_a). When the surface has a curvature as shown in Fig. 3a, the tensile stress across the boundary will be larger than the applied tensile stress by a factor which depends on the position of the boundary along the surface and the geometry of the surface.^(13,14) This stress concentration factor (k) is largest at the position where $\theta = 0$ as shown in Fig. 3a. At this position the tensile stress is

$$\sigma = k \sigma_a \quad (10)$$

The factor k depends on the geometry of the surface, its position (i.e., external or internal surface) and the mode of loading.⁽¹⁴⁾ This stress decreases with increasing distance from the surface into the body. When the dimension of the boundaries are much smaller than the dimensions that define the surface curvature, the tensile stress across the boundary can be approximated by Eq. (10). Thus, the strain rate exhibited by the grain pair at the location shown in Fig. 3a is

$$\dot{\epsilon} = \frac{2\pi x^3 s^5}{3(x+1)\eta s_0^5} k \sigma_a . \quad (11)$$

A crack is also a free surface and a stress concentrator.

The tensile stress distribution in the near vicinity of the crack front, along the symmetry plane for the mode of loading shown in Fig. 3b is⁽¹⁵⁾

$$\sigma = \frac{Y \sigma_a c^{1/2}}{(2r)^{1/2}}, \quad (12)$$

where c is the crack length and r is the distance from the crack front into the material; Y is a dimensionless factor. Since this expression exhibits a singularity* at $r = 0$, it presents a problem in defining the average stress acting across the grain boundary shown in Fig. 3b. For the purposes of this argument, it will be assumed that the average stress is $\sigma = \sigma_a c^{1/2}/D^{1/2}$. Substituting this expression into Eq. (5), the strain rate for a favorably oriented grain pair at the crack front is

$$\dot{\epsilon} = \frac{2\pi x^3 s^5 Y}{3(x+1)\eta s_0^5} \left(\frac{c}{D}\right)^{1/2} \sigma_a \quad (13)$$

In summary, it can be seen that the deformation rate of a grain pair depends on its location. The position of greatest tensile stress is at a crack front; thus grain pairs located at a crack front (or, as discussed in the next section, in the vicinity of crack fronts) will exhibit the greatest deformation rate. Grain pairs located along

* Equation (12) was derived assuming that the two surfaces meeting at the crack front to define a cusp.⁽¹⁵⁾ As discussed in the next section, the radius of curvature at the crack front is finite due to the vapor-liquid surface at the grain boundaries. Thus, the stress distribution at the crack front is somewhat different than given by Eq. (12).

either surface notches or internal cavities* will exhibit the next largest deformation rates. Next in order are grain pairs on planar surfaces and those remote to any surface (assuming $\sigma_a > \sigma_c$).

* Stress concentrators not associated with vapor-liquid surfaces, viz., solid, second phase inhomogeneous, will have a similar effect on grain pairs.

6. DEFORMATION ZONES

In the last section, the effect of stress concentrators was only discussed in relation to grain pairs located on a free surface.

The effect of the stress distribution in the vicinity of these concentrators, away from the free surface was neglected. In this section, the expected zone of deformation associated with the stress distribution around cracks and the expected change in geometry of pre-existing, large cavities will be discussed.

Assume that all boundaries within the ideal polycrystal contain vapor bubbles of size d_0 . Whenever the tensile stress across these boundaries is $\geq \sigma_c$ (see Section 4), boundary separation can take place and these grain pairs can contribute to the total deformation of the material. If the applied stress $\sigma_a < \sigma_c$, only those boundaries around stress concentrators will separate. For the case of a crack, only a certain volume of material in the vicinity of the crack front will satisfy this condition. This volume can be defined by a limiting radius vector r_{lim} as shown in Fig. 4. An approximate equation for r_{lim} can be obtained from Eq. (12) but setting $\sigma = \sigma_c$; thus,

$$r_{lim} \approx \left(\frac{\sigma}{\sigma_c} \right)^2 a \quad (14)$$

This equation shows that when $\sigma_a < \sigma_c$, only those boundaries within a cylindrical volume defined by r_{lim} , with an origin at the crack front, will

separate. Boundaries closest to the crack front will exhibit the greatest separation rate. This, is also true when $\sigma_a > \sigma_c$.

It should be noted here that in a polycrystal with a liquid boundary phase, the crack front is not cusp-shaped as usually assumed, but it has a finite radius of curvature defined by the vapor-liquid interface between the grain pairs at the crack front (see Fig. 3b). Thus, the stress concentration will be somewhat smaller than that usually reported for a sharp crack. As the grains at the crack front separate, the radius of curvature will increase as the vapor-liquid surface propagates to extend the crack's length. It is important to recognize that the curvature cannot be increased by the deformation of adjacent grains as for the case of dislocation motion in most metals, but that it remains small due to limited amount of liquid between the separating grains. Thus, as boundary separation occurs at the crack front, the crack front extends without a significant change in the stress concentration despite the non-elastic deformation in the surrounding material.

As the crack front grows due to successive boundary separation at the crack front, the radius of the deformation zone will increase linearly with c as shown in Fig. 4b. For the case where $\sigma_a > \sigma_c$, all boundaries within the material will separate, but those within the zone associated with the crack front will exhibit the greatest rate of separation.

The initial deformation zone in the vicinity of other types of stress concentrators will depend on their stress distribution. The stress distributions for spherical and ellipsoidal cavities and surface

notches have been analyzed by Neuber.⁽¹⁴⁾ The initial deformation zone associated with these stress concentrators can be defined in a similar manner used above for the case of a crack. This will not be done here. The important observation concerning these zones is that those boundaries at the position of highest stress (viz., at the surface, where $\theta = 0$ in Fig. 3a) will exhibit the greatest separation rate. Thus, after sufficient boundary separation and sliding, a crack will form at the cavity and the stress concentration will become greater.

7. DEFORMATION IN TENSION AND COMPRESSION

Boundaries that are perpendicular to applied compressive forces will move closer together. The liquid between these approaching boundaries must flow to other boundaries which must separate by local tensile stresses. As pointed out in Section 7 the rate of boundary approach ($s/s_0 < 1$) is much smaller than the rate of boundary separation ($s/s_0 > 1$, see Eq. (5)). Thus, one would expect a polycrystal with a liquid boundary phase to be more resistant to deformation during compressive loading than during tensile loading.

If boundary approach was the only phenomenon associated with deformation during compressive loading, one might expect that once all of the liquid between the grains was squeezed out, deformation would stop. This is an unlikely occurrence because boundaries which were separating to accommodate the 'squeezed-out' liquid would continue to separate after the compressed boundaries stopped approaching one another. Also, since the rate of boundary approach is much greater than boundary separation, the mechanics of deformation, due to applied axial compression, can be assumed to be governed by the local tensile stresses which cause boundary separation.

As succinctly reviewed by Babel and Sines,⁽¹⁶⁾ tensile stresses can arise within a body placed in axial (and biaxial) compression. These tensile stresses are located at inhomogeneties,

Preceding page blank

viz., cavities, cracks and second phases. A properly oriented liquid boundary would also qualify as a location for tensile stresses during compressive loading. The tensile stress is largest at specific positions along the surface (or phase boundary) of these inhomogeneities. In general, much larger applied compressive stresses are required to produce the same local tensile stress than required by an applied tensile stress. Since tensile stresses are required for boundary separation, it is important to know the ratio of the applied compressional to the applied tensile stresses to produce the same local stress distribution at an inhomogeneity and thus, the same rate of boundary separation.

The ratio of applied compressional to tensile stresses to produce the same localized tensile stress distribution can be simply illustrated with a derivation borrowed from Babel and Sines.⁽¹⁶⁾ The inhomogeneity used for this derivation is an elliptical hole shown in Fig. 5, which is either placed in compression $(\sigma_a)_{\text{comp}}$ or in tension $(\sigma_a)_{\text{tens}}$ by remote forces. The major axis of the ellipse is oriented such that the largest local tensile stress (σ_t) arises at the same position (shown in Fig. 5) on its surface for both cases of applied stress. The local tensile stress at this position is

$$\sigma_t = \begin{cases} (1 + 2 \frac{a}{b}) (\sigma_a)_{\text{tens}}, & \text{when } (\sigma_a)_{\text{comp}} = 0 \end{cases} \quad (15a)$$

$$\sigma_t = \begin{cases} \frac{(\frac{a}{b} + 1)^2}{4 \frac{a}{b}} (\sigma_a)_{\text{comp}}, & \text{when } (\sigma_a)_{\text{tens}} = 0 \end{cases} \quad (15b)$$

The ratio, $R = (\sigma_a)_{\text{comp}}/(\sigma_a)_{\text{tens}}$ required to produce the same local tensile stress distribution is determined by equating Eqs. (15a) and (15b):

$$R = \frac{4 \frac{a}{b} (1 + 2 \frac{a}{b})}{(1 + \frac{a}{b})^2} . \quad (16)$$

For the case of a cylindrical cavity, $a = b$ and $R = 3$; for the case of a surface crack (or a liquid grain boundary), $\frac{a}{b} \rightarrow \infty$ and $R = 8$. Intermediate values of R are obtained for other a/b ratios. The position of the highest local tensile stress will change as the ellipse is rotated with respect to the directions of applied stresses.

Thus, it can be concluded that if boundary separation limits and governs the deformation behavior of a polycrystalline material, a much larger compressive stress is required (between 3 to 8 times) to produce the same deformation behavior that would be produced by an applied tensile stress.

8. DEFORMATION BEHAVIOR OF POLYCRYSTALS

Up to this section, the main concern has been the deformation behavior of individual and small groups of grain pairs located at specific positions throughout the polycrystalline material. Based on the theory evolved for these localized events, the collective behavior of a polycrystalline body will be discussed.

8.1 Simple Polycrystals

The simplest case to examine is the polycrystalline material consisting of uniform, cube-shaped grains which are initially separated from one another by a liquid phase of thickness s_0 (see Fig. 1). Three cases will be viewed:

- (1) Each boundary contains a vapor bubble of diameter d_0 .
- (2) Occasional boundaries contain bubbles of diameter d_0 . Other boundaries have either smaller diameter bubbles or do not contain bubbles.
- (3) No vapor bubbles are present.

In each case, the long polycrystalline body is fixed at both ends and placed in tension by external forces. Elastic deformation will be neglected.

The first case is illustrated in Fig. 6a. When the applied tensile stress $\sigma_a > \sigma_c$ ($\sigma_c = \frac{4\gamma}{d_0}$, see Section 4), all the boundaries perpendicular to the applied tensile stress will separate at a rate given by Eq. (5). The strain in the direction of applied stress as a function of time* is given by:

$$\epsilon \approx \frac{2\pi x^3 t \sigma}{(x+1)(3\eta - 8\pi x^2 t \sigma)} . \quad (17)$$

For this case, boundary sliding does not occur during deformation, i.e., the body will separate into rows of grains shown in Fig. 6a. The situation where $\sigma_a < \sigma_c$ will be examined as part of case 3.

For the second case, when $\sigma_a > \sigma_c$, only those boundaries perpendicular to the applied tensile stress which contain vapor bubbles of size d_0 will separate. The deformation equation for this case is the same as given for case 1 (Eq. (17)), but the mechanics of deformation require that some boundaries slide as shown in Fig. 6(b).

In the third case (or if $\sigma_a < \sigma_c$ in the previous cases) only the boundaries at the surface, which have a vapor-liquid interface, would be free to separate if it were not for the end constraints which cause the strain throughout a cross-section to be uniform. Because vapor-liquid interfaces are only present on the surface of the body, the separation of the body's cross-section can only occur by the movement of the vapor-liquid interface from its surface to the interior as shown in Fig. 6c.

* It is assumed that the tensile stress across the boundaries is σ_a , i.e., the presence of bubbles and their growth can be neglected in determining the stress at the boundary. This assumption is only valid when $d_0 \ll D$ and ϵ is small.

This is the case of the two grains shown in Fig. 2b. The volume of liquid between the separating surfaces is $V = L^2 s_0$, where L is the diameter of the body, $L = mD$, and m = the number of grains of dimension D . Substituting these relations into Eq. (4), it can be shown that the deformation also depends on m . Since m depends on the cross-sectional size of the body, it can be shown that the deformation behavior for this case depends on the size of the body. For very large bodies, $m \rightarrow \infty$, and the body will not exhibit any non-elastic deformation. The third case could be further extended to the condition where only a few of the boundaries contain vapor bubbles.

Summarizing these three cases for the simplistic polycrystal shown in Fig. 6, it can be seen that the deformation behavior depends on several microstructural features and the flow characteristics of the liquid phase. The microstructural features are the volume fraction of the liquid phase, which governs the initial boundary separation thickness, s_0 (see Appendix A), and the size of vapor bubbles which governs the critical (threshold) stress below which non-elastic deformation will not occur in a practical sense for large bodies. It should be pointed out that the largest vapor bubble size is related to grain size, i.e., $d_{\text{largest}} = s_0 = [V_\ell / (3(1-V_\ell))]D$. Thus, for equivalent materials except grain size, the material with the smallest grain size will have the largest threshold stress for non-elastic deformation.

The flow characteristics of the boundary phase that also govern the deformation behavior depends on the type of phase present. For the

case of a Newtonian boundary phase, the viscosity is the single parameter of interest; for non-Newtonian liquid, Eq. (17) would be modified to include the two parameters, η and n (see Appendix B). The effect of temperature on the deformation behavior can be brought into Eq. (17) through these flow parameters.

8.2 Real Polycrystals

The microstructures of real polycrystals are much more complex than that treated above. Within a polycrystalline material, the grains have different geometries and sizes. The thickness of the liquid boundary will vary from boundary to boundary. Other microstructural features may be present, viz., voids, solid inclusions and cracks. The effect of each of these on the deformation behavior will be briefly discussed.

Different grain geometries will effect the mechanics of deformation. For example, the tensile stress normal to each boundary and the shear stress parallel to each boundary will be different than that assumed above due to different boundary orientations. Without rigorous proof, it might be expected that the effect of grain morphology and size distribution would alter some of the variables in the deformation equation (Eq. (17)), e.g., the relation between s_0 and D will be different from that given in Appendix A, without changing its general form.

Different boundary separations within the same polycrystal will have an effect during the initial period of deformation. Boundaries widely separated by a liquid can act as reservoirs for adjacent, narrow boundaries that are favorably oriented for separation. The flow of

liquid from thick to thin boundaries precludes the need for an unstable vapor bubble. Because the thick boundaries have a potential for separating at a fast rate if they were not constrained by the thin boundaries, the applied tensile stress will be unevenly distributed. That is, the thinner boundaries will carry much of the tensile load, and initially, they will separate at a much greater rate than that given by Eq. (17). Once all the boundaries have reached an equilibrium separation distance to produce a uniform tensile stress distribution, the flow of liquid from boundary to boundary will stop as discussed in Section 3. After this initial period, the deformation behavior should be similar to that given by Eq. (17).

Microstructural features such as large voids, solid inclusions and pre-existing cracks might be expected to result in the largest deviation from the deformation behavior given by Eq. (17). These heterogeneously distributed positions of high tensile stress will result in zones of higher deformation than found in volume elements remote from these positions. As discussed in Section 6, the voids and solid inclusions will form internal cracks. These cracks, together with pre-existing cracks, will slowly grow to change the compliance of the body and thus, contribute to the total non-elastic strain.

Figure 7 illustrates that cracks do grow during deformation and contribute to the total strain in materials that contain a viscous boundary phase. The 4-point flexural creep specimen shown in this figure was made from hot-pressed Si_3N_4 , which is believed to contain a viscous

boundary phase* at high temperatures. The experiment was conducted at 1400°C with a constant moment of 1.03 MN/m (corresponding to an initial stress of 105 MN/m²). After a period of 6 hrs. in the range where the specimen exhibited a constant deformation rate, it was cooled. When the oxide surface layer was removed, many large cracks could be observed extending from the tensile to the compression surface. Small cracks which could not be photographed, were also present. Such large cracks would significantly effect the compliance of the specimen. The large separation distance between the crack surfaces at the tensile surface is evidence for a large deformation zone at the crack front.

In summary, the deformation behavior of a polycrystalline material with a viscous boundary phase is governed by the rate that boundaries can separate. Boundary sliding is important to the mechanics of deformation, but it is not a limiting step. The important parameters of the boundary phase are its flow characteristics and its volume content. Important microstructural features of the polycrystal are (1) vapor bubbles within the boundary phase, which are necessary for boundary separation; (2) grain size, which governs the largest bubble size and thus, the threshold tensile stress below which deformation will not occur; and (3) inhomogeneities, viz., voids, solid inclusions and cracks, which result in deformation zones and the slow growth of cracks that change the compliance of the body and add to the total non-elastic

*As discussed elsewhere, (17) impurities such as CaO are believed to strongly effect the viscosity of the boundary phase. The Si₃N₄ material used for this experiment was relatively impure and thus exhibited greater deformation than purer forms of Si₃N₄.

strain. Polycrystalline materials with a viscous boundary phase will exhibit a much greater rate of deformation in tension than in compression. The different deformation behaviors in tension and compression is the best and most convenient way of differentiating grain separation due to a viscous boundary phase from other mechanisms (viz., diffusion and dislocation phenomenon) that can control deformation. It should also be noted that deformation by boundary sliding is not a plastic phenomenon since volume is not conserved.

APPENDIX A: RELATION BETWEEN BOUNDARY THICKNESS, GRAIN
SIZE AND VOLUME CONTENT OF LIQUID PHASE

If it is assumed that the polycrystalline body is composed of cube-shaped grains with an edge dimension, D , uniformly separated by a liquid phase of thickness s_0 , the volume fraction of the liquid (V_L) is given by

$$V_L = \frac{(D + s_0)^3 - D^3}{(D + s_0)^3} . \quad (1a)$$

By letting $s_0 = x D$, this expression can be rewritten as

$$V_L = \frac{3x + 3x^2 + x^3}{1 + 3x + 3x^2 + x^3} . \quad (2a)$$

Since the liquid is considered a minor phase, viz., $x < 0.1$, higher order terms of x can be neglected resulting in

$$x = \frac{V_L}{3(1 - V_L)} . \quad (3a)$$

APPENDIX B: DEFORMATION RATE OF GRAIN PAIRS SEPARATED BY
EITHER A NON-NEWTONIAN LIQUID OR A BINGHAM SOLID

The deformation rate ($\dot{\epsilon}$) of a quasi-plastic phase is defined by

$$\dot{\epsilon} = \frac{(\tau - \tau_0)n}{\eta} ,$$

where τ = an applied shear stress, τ_0 = a yield shear stress, η = viscosity and n = a positive numerical constant. When $n = 1$ and $\tau_0 = 0$, the phase is a Newtonian liquid and when $n > 1$, $\tau_0 = 0$, a non-Newtonian liquid. A Bingham solid is defined by $n = 1$ and $\tau_0 > 0$.

The separation rate of parallel plates initially separated by a quasi-plastic phase of thickness s_0 has been analyzed by Scott.[18] He obtained solutions for the cases of a non-Newtonian liquid and a Bingham solid. Using the definitions established in Section 2 of the text, the rate of deformation of a grain pair containing either of these phases is given by

(a) Non-Newtonian liquid separating grains:

$$\dot{\epsilon} = \frac{(3n+1)^n \pi^{n+1/2} x^{n+2}}{(2nn)^n (n+2) (x+1)} \left(\frac{s}{s_0}\right) \frac{5n+5/2}{\sigma^n}$$

(b) Bingham solid separating grains:

$$\dot{\epsilon} = \frac{2\pi x^3}{3\eta(x+1)} \left(1 + \frac{1}{2} \left(\frac{s}{s_L}\right)^{-15/2}\right) \left(\frac{s}{s_0}\right)^5 \sigma - \frac{2\pi^{1/2} x^2}{3\eta(x+1)} \left(\frac{s}{s_0}\right)^{5/2} \tau_0$$

where

$$s_L = \left(\frac{4 s_0 \tau_0^2}{4\pi x^2 \sigma^2} \right)^{1/5}$$

Scott [18] also points out that boundaries separated with a Bingham solid cannot be made to approach one another by any distance $< s_L$.

ACKNOWLEDGMENTS

Great thanks is due to Professor W. R. Bitler who patiently reviewed the concepts in this article. One of his criticisms resulted in a better conceptual view of the stress concentration at a crack as related to the finite radius of curvature of the vapor-liquid surface between the grain pairs at the crack front and the change of this curvature during crack growth (see Section 6). Thanks are also due to Dr. A. M. Diness who suggested my involvement in deformation.

REFERENCES

1. Mechanical Behavior of Materials at Elevated Temperatures, Ed. by J. E. Dorn, McGraw-Hill (1961).
2. G. R. Terwilliger and K. C. Radford, "High Temperature Deformation of Ceramics: I, Background", Bul. Amer. Ceram. Soc., 53, 172 (1974).
3. R. Raj and M. F. Ashby, "On Grain Boundary Sliding and Diffusional Creep", Trans. Met. Soc. AlME 2, 1113 (1971).
4. For example, F. W. Sears and M. W. Zemansky, College Physics, Addison-Wesley, p. 254 (1952).
5. N. A. DeBruyne, "The Measurement of the Strength of Adhesive and Cohesive Joints", Adhesion and Cohesion, Ed. by P. Weiss, Elsevier, p. 55 (1962).
6. D. Tabor, "Friction and Adhesion Between Metals and Other Solids", Adhesion, Ed. by D. D. Eley, Oxford, p. 118 (1961).
7. J. Hoekstra and C. P. Fritzius, "Rheology of Adhesives", Adhesion and Adhesives, Ed. by N. A. DeBruyne and R. Jouwink, Elsevier, p. 63 (1951).
8. A. Healey, Trans. Inst. Rubber Ind. 1, 334 (1926).
9. J. Stefan, Sitzungsberichte Kaiserl. Akad. Wiss. Wien, math. natur. klasse, 69, 713 (1874).
10. J. C. Fisher, "The Fracture of Liquids", J. Appl. Phys., 19, 1062 (1948).

Preceding page blank

11. A. A. Griffith, "Phenomena of Rupture and Flow in Solids", Phil. Trans. Roy. Soc. London, Ser. A. 221, 163 (1920).
12. G. W. Morey, "The Property of Glass", p. 197-211, Reinhold (1938).
13. C. E. Inglis, "Stresses in a Plate due to the Presence of Cracks and Sharp Corners", Inst. Naval Archit. 55, 219 (1913).
14. H. Neuber, Theory of Notch Stresses, 2nd Edition, Springer (1958). (English Trans. available from Office of Technical Service Dept., Commerce, Washington, D. C.).
15. I. N. Sneddon, "The Distribution of Stress in the Neighborhood of a Crack in an Elastic Solid", Proc. Roy. Soc. Lond. 187, 229 (1946).
16. H. W. Babel and G. Sines, "A Biaxial Fracture Criterion for Porous Brittle Materials", Trans. ASME, J. Basic Eng., 285 (1968)
17. F. F. Lange and J. L. Iskoe, "High Temperature Strength Behavior of Hot-Pressed Si_3N_4 and SiC: Effect of Impurities", Proc. Army Mat. Tech. Conf. on Ceramics for High Performance Applications (in press).
18. J. R. Scott, "Theory and Application of the Parallel-Plate Plastimeter", Trans. Inst. Rubber Ind. 7, 169 (1931).

Dwg. 6234A48

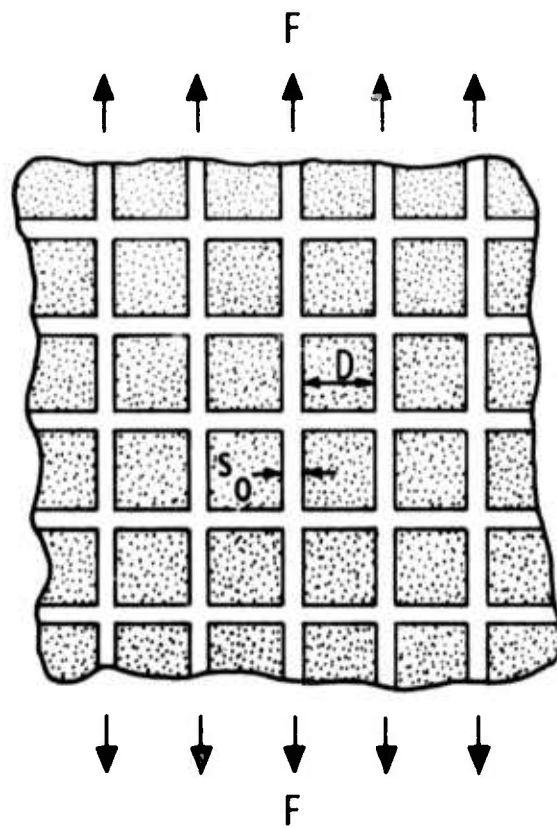


Fig. 1

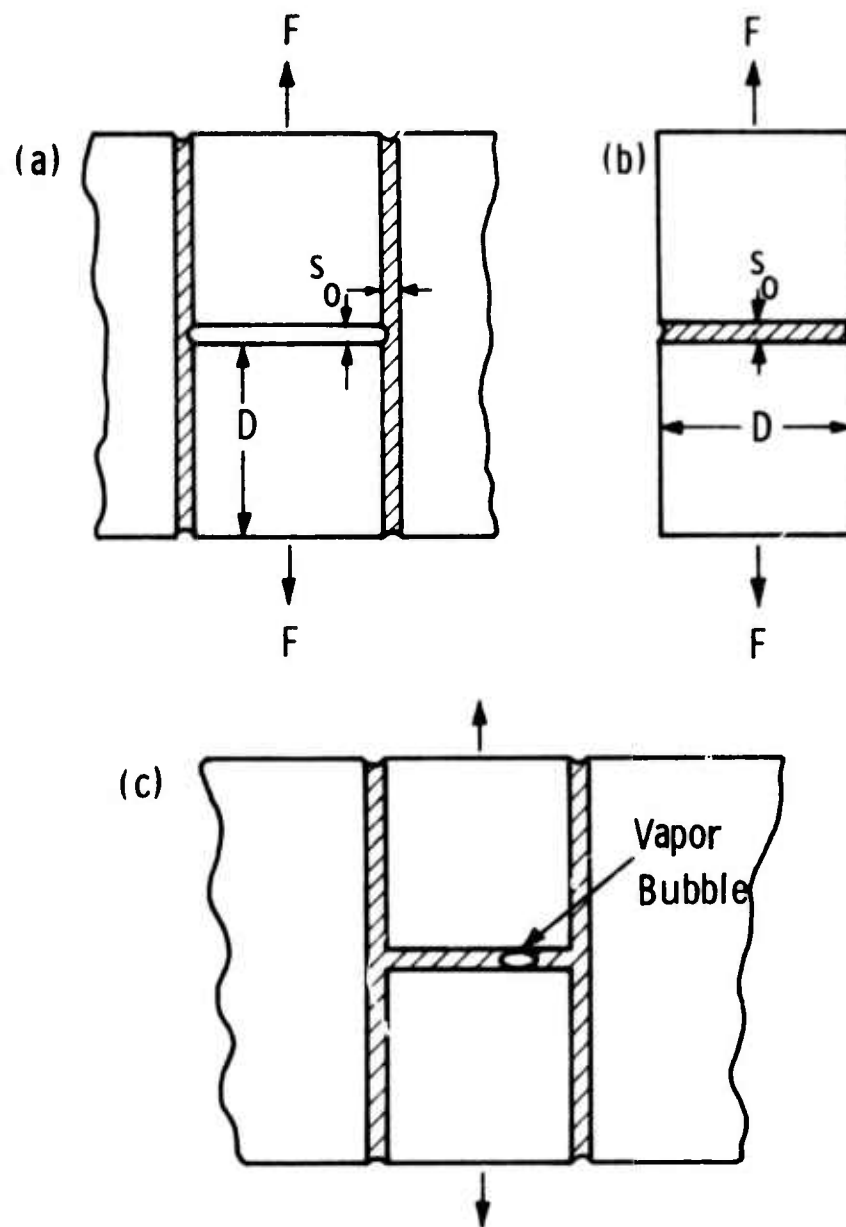


Fig. 2

Dwg. 6234A46

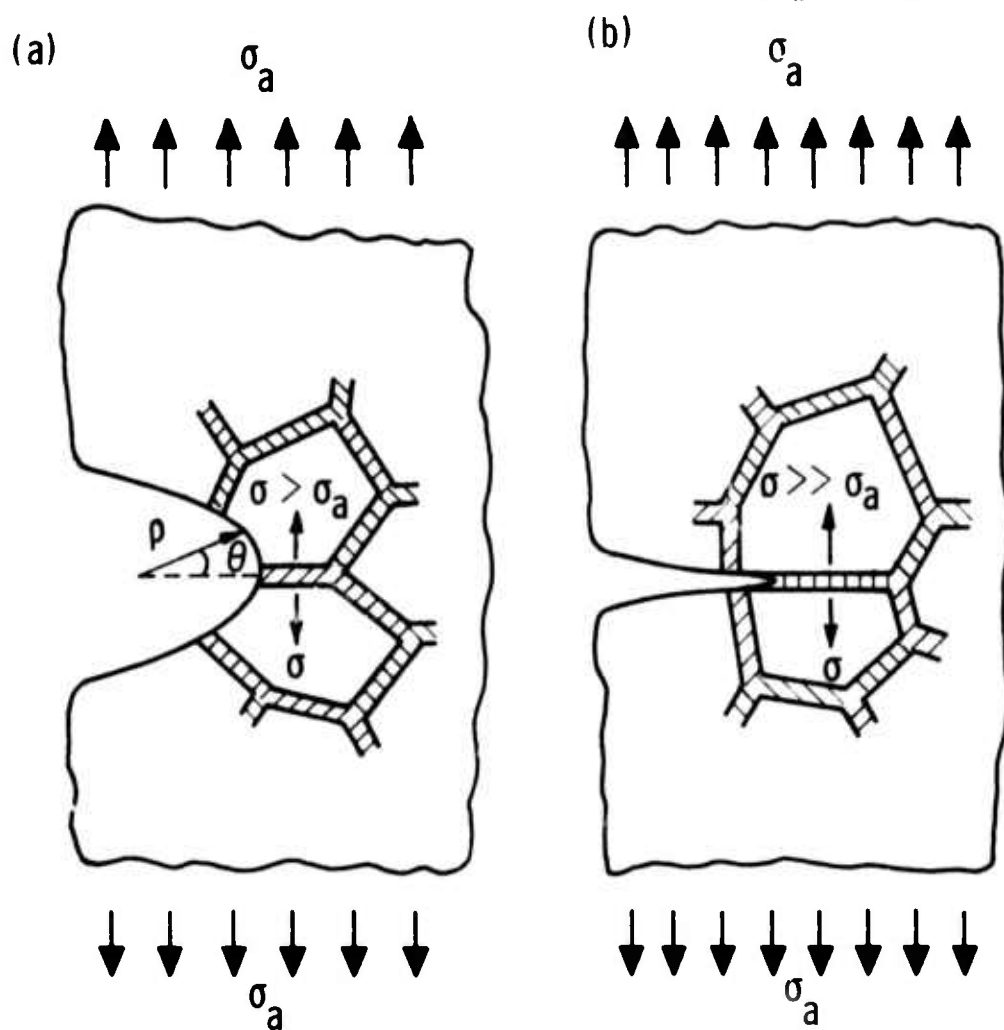


Fig. 3

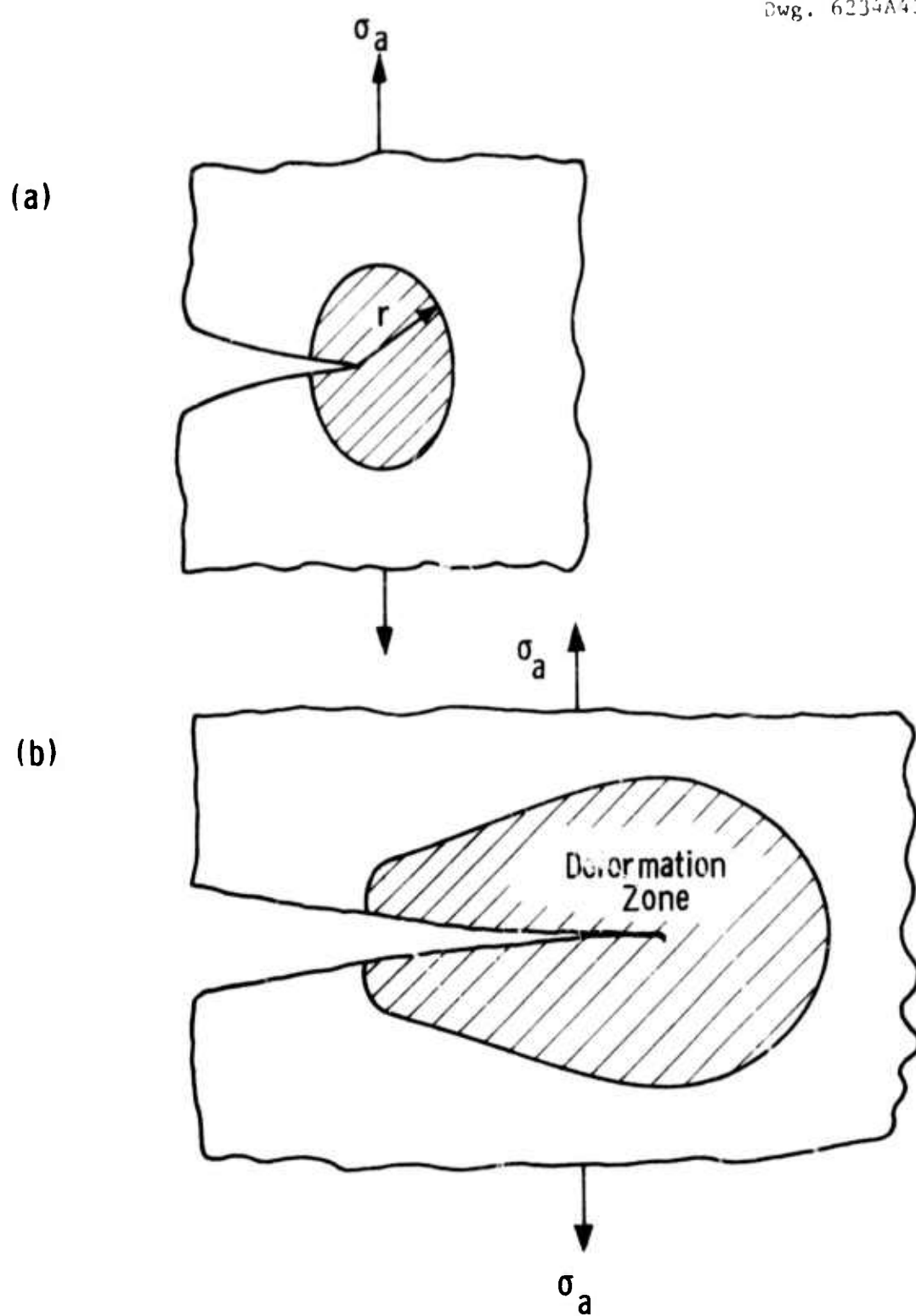


Fig. 4

- 4.2 -

Dwg. 6234A50

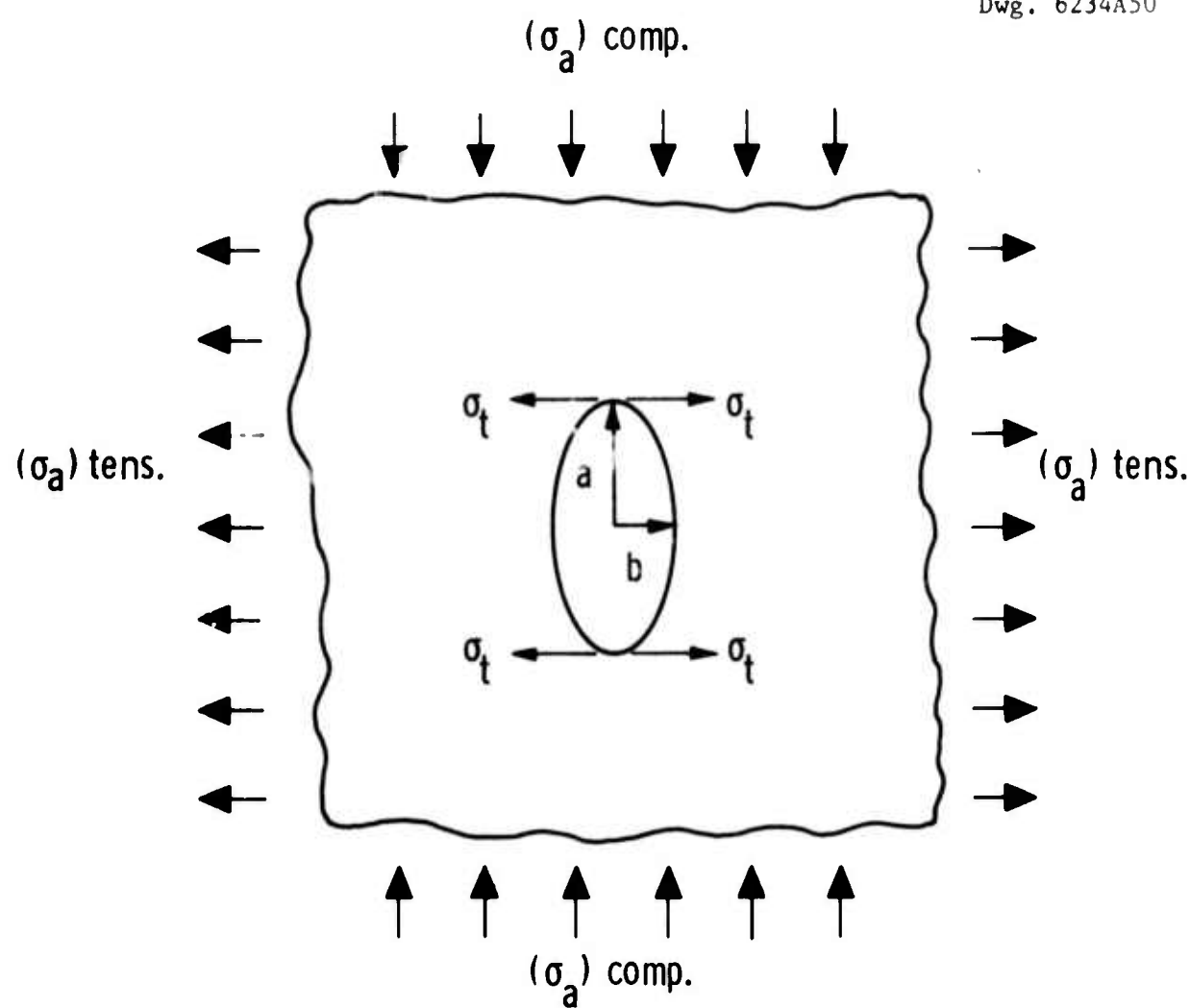


Fig. 5

- 43 -

Dwg. 6234A49

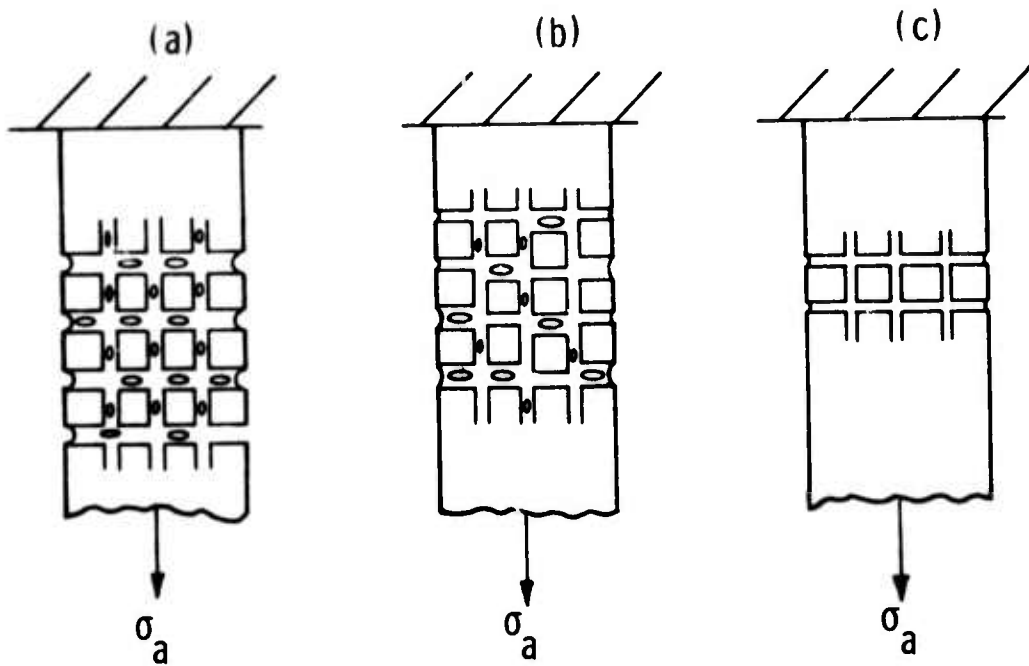


Fig. 6

tensile surface with cracks



compressive ↑ surface

FIG. 7

- 45 -